

# A simplified model for the fabrication of silver nanowires in a continuous flow process and its experimental verification

Grzegorz Dzido<sup>1\*</sup> , Muhammad Omer Farooq<sup>2</sup> , Aleksandra Smolska<sup>2</sup> 

<sup>1</sup> Silesian University of Technology, Department of Chemical Engineering and Process Design, Strzody 7, 44-100 Gliwice, Poland

<sup>2</sup> Silesian University of Technology, Doctoral School, Akademicka 2A, 44-100 Gliwice, Poland

## \* Corresponding author:

e-mail:

[grzegorz.dzido@polsl.pl](mailto:grzegorz.dzido@polsl.pl)

Presented at 24th Polish Conference of Chemical and Process Engineering, 13–16 June 2023, Szczecin, Poland.

## Article info:

Received: 28 April 2023

Revised: 15 July 2023

Accepted: 16 July 2023

## Abstract

The publication presents experimental verification of a mathematical model of silver nanowire (AgNWs) fabrication in a continuous flow process in a helical tubular reactor. Silver nanowires were synthesised with a polyol process, with ethylene glycol as the reductant of the nanomaterial precursor and solvent of the reactants. The observed average diameters and lengths of AgNWs were 98–226 nm and 5–45  $\mu\text{m}$ , respectively. The experimental conversions of the precursor were 0.71–0.90. A comparison of calculated and measured conversions for the investigated range of residence times and temperatures showed that the observed error was less than 20%.

## Keywords

continuous flow synthesis, silver nanowires, polyol process

## 1. INTRODUCTION

Silver nanowires, defined as nanostructures with an average diameter of 10–200 nm and length of 5–100  $\mu\text{m}$  (Ha et al., 2022), are intensively investigated regarding their application and fabrication methods. The growing demand for nanomaterials is prompting the search for new production methods. Nanowires can be produced using the so-called hard and soft template methods. The latter is most often used to produce silver nanowires in the polyol process, in which polyhydric alcohol is both a reductant of the nanomaterial precursor and a solvent for the reactants. The embryos formed in the initial stage of the process undergo further unidirectional growth due to the use of a capping agent, which is usually polyvinylpyrrolidone (PVP). Adsorbing onto the surfaces of crystallites with the highest surface energy {100}, presence of PVP promotes one-directional growth by selectively extending lower energy facets {111}. It was experimentally demonstrated that the average molecular weight of PVP significantly affected the length of the discussed nanostructures (Zeng et al., 2014). An additional factor influencing the intensification of the synthesis of AgNWs is a mediating agent responsible for stabilising the nuclei, buffering the concentration of silver cations and binding atomic oxygen, the presence of which negatively affects the development of nanowires. Inorganic compounds that are metal chlorides or bromides are most commonly used as mediating agents (Nandikonda and Davis, 2011). The selection of the concentrations of the discussed compounds affects the length and diameter of AgNWs and the presence of a by-product in the form of silver crystals of various morphology.

While the methods for realising batch-mode chemical syntheses are relatively well recognised, there is still insufficient

data for processes carried out in the flow mode. There are few publications in the open literature on the synthesis in question, which mainly focus on the qualitative description of the product and its potential application (Espinosa et al., 2016; Gottesman et al., 2012; Yu et al., 2022). More detailed quantitative data concerning flow characteristics and temperature distribution in the reactor can be found in the works of Chou et al. (2015) and Hemmati et al. (2017).

The relatively small number of papers on the fabrication of silver nanowires in a continuous flow process provided the rationale for the research. This paper presents a simplified mathematical model to determine changes in basic process parameters along the flow path through a convection-heated tubular reactor and its experimental verification regarding the final conversion of the nanomaterial precursor and outlet temperature. Syntheses of AgNWs were carried out using polyvinylpyrrolidone (PVP) of different molar masses as the stabiliser. Copper (II) chloride was used as the mediating agent. Due to its relatively low toxicity and easy availability, this substance is commonly used to fabricate AgNWs discussed here. Copper present in the molecule of  $\text{CuCl}_2$ , which can have two oxidation stages, makes this substance an effective oxygen scavenger.

## 2. MODEL OF THE PROCESS

The mathematical model used in the process analysis was based on equations describing the steady-state transport of heat from the environment where the helical tubular reactor was located to the flowing reaction mixture:

$$\dot{Q} = \dot{G}_{Cp} (t_i - t_0), \quad (1)$$



$$\dot{Q} = \alpha_{ge} \pi d l_i (t_w - t_i), \quad (2)$$

$$\dot{Q} = \alpha_p \pi d_z l_i (t_p - t_{wz}) \quad (3)$$

Equation (4) considers the thermal resistances occurring during heat transfer in a reactor made of a thick-walled silicon tube:

$$\dot{Q} = \left( \frac{1}{\alpha_p d_z} + \frac{1}{2\lambda_t} \ln \left( \frac{d_z}{d} \right) + \frac{1}{\alpha_{ge} d} \right)^{-1} \pi l_i (t_p - t_i) \quad (4)$$

The heat transfer coefficient to the outer surface of the tubular reactor  $\alpha_p$  was assumed to be the sum of constituents considering free convection  $\alpha_c$  and radiation  $\alpha_r$ . It was evaluated according to simplified equations developed for air (Senkara, 1981; Hobler, 1979):

$$\alpha_p = \alpha_c + \alpha_r = 2.56 (t_p - t_{wz})^{0.25} + 4\sigma\varepsilon_z \left( \frac{(t_p + 273) + (t_{wz} + 273)}{2} \right)^3 \quad (5)$$

where equivalent emissivity  $\varepsilon_z$  was calculated as:

$$\varepsilon_z = \frac{1}{\frac{1}{\varepsilon_1} + \frac{F_1}{F_2} \left( \frac{1}{\varepsilon_2} - 1 \right)} \quad (6)$$

assuming the emissivity of silicone rubber  $\varepsilon_1 = 0.9$  and internal radiating elements of dryer  $\varepsilon_2 = 0.8$ . The ratio of absorbing to radiation-emitting surfaces ( $F_1/F_2$ ) was assumed to equal 0.1.

The heat transfer coefficient for a reaction mixture flowing laminarily in the helical reactor was calculated using the equation (Manlapaz and Churchill, 1981):

$$\text{Nu} = \frac{\alpha_{ge} d}{\lambda} = \left[ \left[ 3.657 + \frac{4.343}{1 + \frac{\text{Pr He}^2}{957}} \right]^3 + 1.158 \left( \frac{\text{He}}{1 + \frac{\text{Pr}}{0.477}} \right)^{\frac{3}{2}} \right]^{\frac{1}{3}} \quad (7)$$

where:

$$\text{He} = \text{Re} \sqrt{\frac{d}{D \left( 1 + \frac{\rho}{\pi D} \right)}} \quad (8)$$

Preliminary calculations showed that the Reynolds number value in the reactor was 0.5–1.9.

Due to the low concentration of the reaction mixture, the physical properties were assumed in the calculations as for pure ethylene glycol. They were estimated for the arithmetic average temperature between the inlet and the cross-section corresponding to the  $l_i$  coordinate using the equations implemented in ChemCAD™ (Chemstations, USA).

The concentration profile of AgNWs precursor along the reactor was described using the following equation:

$$C_A = C_{A0} \exp \left( -l_i \frac{k}{u} \right) = C_{A0} \exp \left( -l_i \frac{k_0}{u} \exp \left( -\frac{E_A}{R(t_i + 273)} \right) \right) \quad (9)$$

The equation was derived based on the assumption of uniform flow through the tubular reactor (Doran, 2013). In the calculations, it was assumed that the course of the AgNWs production process is limited by the rate of monomer (silver atoms) production and is subject to pseudo-first-order reaction kinetics ( $(-r_A) = kC_A$ ). It is justified by the significant excess of reductant relative to the precursor used. The temperature dependence of the reaction rate was described using the Arrhenius equation. In this equation, the activation energy was assumed to be  $E_A = 54000$  J/mol, based on literature data (Zhai and Efrima, 1996) derived from theoretical considerations on silver nanoparticle nucleation. The pre-exponential factor  $k_0 = 6000$  1/s was selected experimentally to minimise the sum of squares of the deviations between calculated and observed conversion values for 12 observations. Noteworthy, this magnitude is close to that which was determined experimentally during investigations of the kinetics of silver nanoparticle preparation in the polyol process (Dzido, 2017).

For given values of  $l_i$ , the system of equations (1)–(4) and (9) was solved against the unknowns  $Q$ ,  $t_i$ ,  $t_w$ ,  $t_{wz}$  and  $C_A$  using the Levenberg-Marquardt algorithm implemented in the MathCAD™ 15 (PTC Inc., USA). Calculations were carried out for the residence times of 10, 20 and 30 min,  $t_{in} = 27$ – $38$  °C and  $t_p = 170$ – $180$  °C corresponding to the experimental conditions. The residence time inside the reactor was calculated as follows:

$$\tau = \frac{V}{\dot{V}} \quad (10)$$

### 3. EXPERIMENTAL VERIFICATION OF THE MODEL

The syntheses were carried out using  $\text{AgNO}_3$  as a precursor of AgNWs, at a reactor inlet concentration of  $C_{A0} = 16.8$  mM. Polyvinylpyrrolidone was applied as the capping agent with an average molar mass of 40 kDa (PVP A), 360 kDa (PVP B) and 1300 kDa (PVP C). The typical synthesis used 120 cm<sup>3</sup> of ethylene glycol, which was the solvent for the substrates. As a mediating agent,  $\text{CuCl}_2$  was used. Preliminary experiments made it possible to determine the working concentrations of mediating and stabilising agents, enabling them to be used in a continuous flow process. A reasonable residence time and the possibility of producing a nanomaterial with the highest possible aspect ratio were used as selection criteria. For  $\text{CuCl}_2$ , the concentration was 0.11 mM. During the syntheses, PVP was used in such an amount that

[PVP]:[Ag<sup>+</sup>] = 3 was satisfied, where the concentration of PVP was related to the monomer molecular mass.

Experiments were carried out using the system shown in Fig. 1. The reaction mixture was provided with a syringe pump NE-100 (NEPS, USA) (1) to a helical tubular reactor ( $D = 0,063$  m) (3) located inside a laboratory dryer (2). A reactor was made of a 2.310 m long silicon tube with an outer and inner diameter equal to  $d_z = 0.009$  m and  $d = 0.003$  m, respectively, wound around a glass tube with an outer diameter of 0.054 m. The reaction mixture was collected in a vessel (4) and cooled to room temperature. It was then purified and separated by five-fold centrifugation and washing with DI water using a Hermle Z36HK (Hermle, Germany) centrifuge. Centrifugation was carried out at the rate of 4200 1/min for 20 min. This rate ensures the separation of AgNWs from silver nanoparticles and most of the smaller objects in the reaction mixture and, at the same time, prevents damage to the nanowires by breaking, bending or clustering them into larger clusters. Inlet and outlet reactor temperatures ranged  $t_0 = 27\text{--}38^\circ\text{C}$  and  $t_{\text{out}} = 174\text{--}183^\circ\text{C}$ , respectively, and were measured using two K-type thermocouples connected to the digital thermometer YC-747UD (Maxthermo-Gitta, Taiwan). During experiments, the laboratory dryer was preset to  $t_p = 170^\circ\text{C}$  or  $180^\circ\text{C}$ . The volumetric flow rate of the reaction mixture was adjusted to achieve assumed residence times.

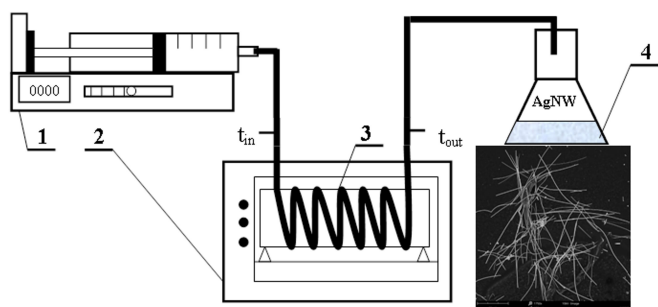


Figure 1. Laboratory setup for AgNWs fabrication: 1 – syringe pump, 2 – laboratory dryer, 3 – a helical tubular reactor, 4 – product container.

Silver nanowire precursor conversion was determined by measuring the concentration of Ag<sup>+</sup> ions with an EAg/S-01 ion-selective electrode (Hydromet, Poland) in the post-reaction mixture and calculated as:

$$X = \frac{C_{A0} - C_{Aout}}{C_{A0}} \quad (11)$$

The conversion calculated in this way considers the total precursor consumption for fabricating AgNWs and silver nanoparticles.

The morphology of fabricated materials was examined with an SEM microscope, Phenom ProX (ThermoFisher Scientific, USA), working at an accelerating voltage of 10 kV. Investigation of the crystalline phase was carried out on

a Seifert 3003TT (Agfa–Seifert, Germany) diffractometer using Cu K $\alpha$  radiation ( $\lambda = 0.1540598$  nm) in the  $2\theta$  range  $30\text{--}80^\circ$  with a step size of  $0.05^\circ$ . To determine the average diameter and length of AgNWs, 30 objects in SEM images were analysed using ImageJ software.

## 4. RESULTS AND DISCUSSION

Figures 2a–i show SEM images of selected AgNWs samples synthesised in the continuous flow process for different residence times, temperatures inside the dryer and capping agents used. In all cases under analysis, an increase in conversion accompanying an extension of the residence time in the reactor can be observed. A rise in temperature outside the reactor from  $t_p = 170$  to  $180^\circ\text{C}$  induces a moderate enhancement of conversion with an associated decrease in average nanowire length and increase in diameter for the same capping agent (Figs 2a, b, c and 2g, h, i). The decrease in the viscosity of the environment induced by the increase in temperature, according to the Stokes–Einstein equation, leads to a reduction in the diffusion resistance for the transport of Ag<sup>0</sup> monomers necessary for the expansion of the nanowire planes. It is particularly true of the lateral surfaces of AgNW, with the highest surface energy (Chen et al., 2010), and provides a plausible explanation for the observed increase in diameters at the expense of the expansion of their length. The use of the capping agent with higher molecular weight PVP B (Figs. 2d,e,f) induced an increase of the average length and diameter of the synthesised AgNWs in most analysed cases compared to the results obtained with PVP A. The use of the capping agent with the highest molecular weight (PVP C) led to a significant decrease in the length of AgNWs, 5–10  $\mu\text{m}$ , while maintaining diameters in the 109–120 nm range (not shown in Fig. 2). It is likely that the use of the stabiliser with the most extended polymer chains can significantly hinder the transport of silver atoms to the expanding surfaces of the formed nanomaterial.

X-ray diffraction (XRD) analysis was applied to assess the structure of a selected sample of AgNWs. Figure 3 presents a typical XRD spectrum for AgNWs manufactured with ethylene glycol as reductant at  $\tau = 30$  min and  $t_p = 170^\circ\text{C}$ . Diffraction peaks occurring at  $2\Theta = 38.10, 44.25, 64.35$  and  $77.35^\circ$  correspond with peaks which describe bulk silver (ICSD card No. 01-071-6549). They can be attributed to crystallographic planes (111), (200), (220) and (311) of face-centred cubic silver crystals. The observed (111) to (200) intensity of reflexes ratio amounts to 3.7 (Fig. 3) and it exceeds the theoretical value of 2.2 (ICSD sheet No. 01-071-6549). It points to a considerable quantity of (111) crystal planes in the sample examined and a preferential direction of growth of one-dimensional silver nanostructures (Luu et al., 2011).

Figures 4a, b, c and 4d show graphical results obtained by solving equations modelling the process of AgNWs fabrica-

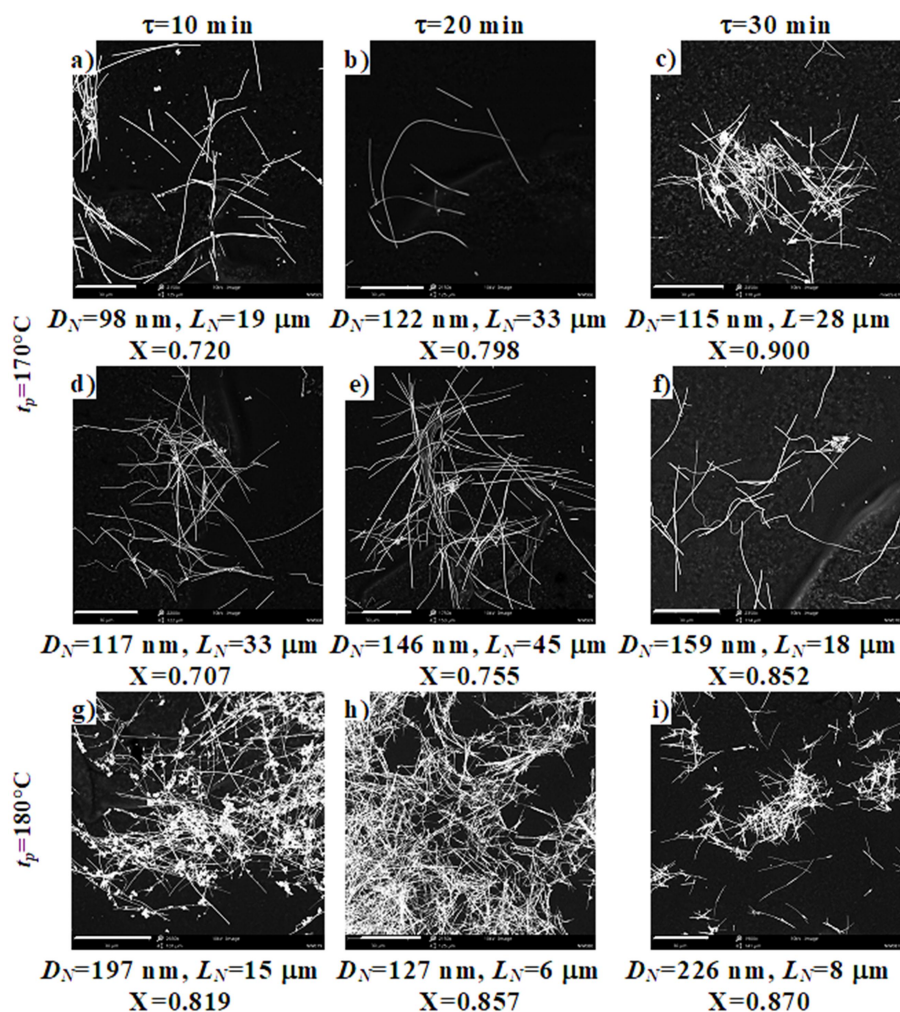


Figure 2. SEM images of AgNWs fabricated in continuous flow polyol process: a), b), c) PVP A; d), e), f) PVP B; g), h), i) PVP A.  $D_N$ , and  $L_N$  stand for average diameter and length, respectively. The scale bar in all cases is 30  $\mu$ m.

tion in a tubular reactor for parameters used in the syntheses mentioned above. Figure 4a shows the effect of residence

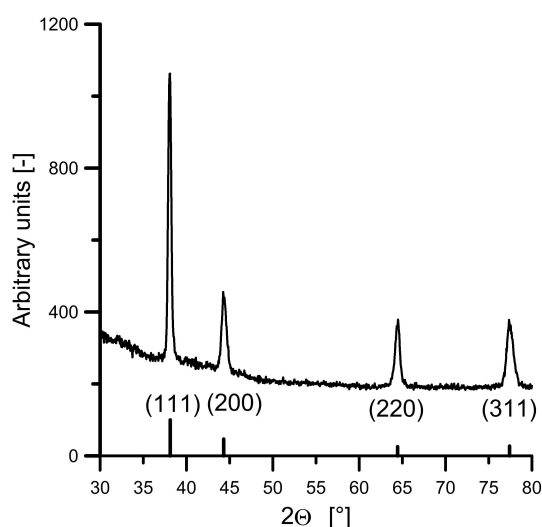


Figure 3. XRD spectra for sample of AgNWs fabricated at  $\tau = 30$  min and  $t_p = 170^\circ\text{C}$ .

time in the reactor on the temperature evolution of the reaction mixture. A characteristic feature of the obtained temperature profiles is the observed rapid increase of liquid temperature in the initial section of the reactor, about 0.25 m. At a later stage, temperature gradually rises towards the temperature resulting from the preset temperature inside the dryer  $t_p = 170^\circ\text{C}$ . A similar course is presented in Fig. 4b, showing temperature profiles inside the reactor for different settings in the dryer;  $t_p = 170$  and  $180^\circ\text{C}$ .

Figures 4c and 4d illustrate the predicted course of changes in precursor concentration and associated conversion changes for different residence times. A short entrance region of approximately 0.25 m can be observed near the inlet to the reactor, where changes in precursor concentration are limited. It results from relatively low temperature in this zone and consequently slows the reaction rate. This effect is particularly pronounced for the lowest residence time  $\tau = 10$  min. Further away from the reactor inlet, changes are increasingly steeper, and for residence times  $\tau = 20$  and 30 min, a trend towards stabilisation of concentration and conversion changes is ob-

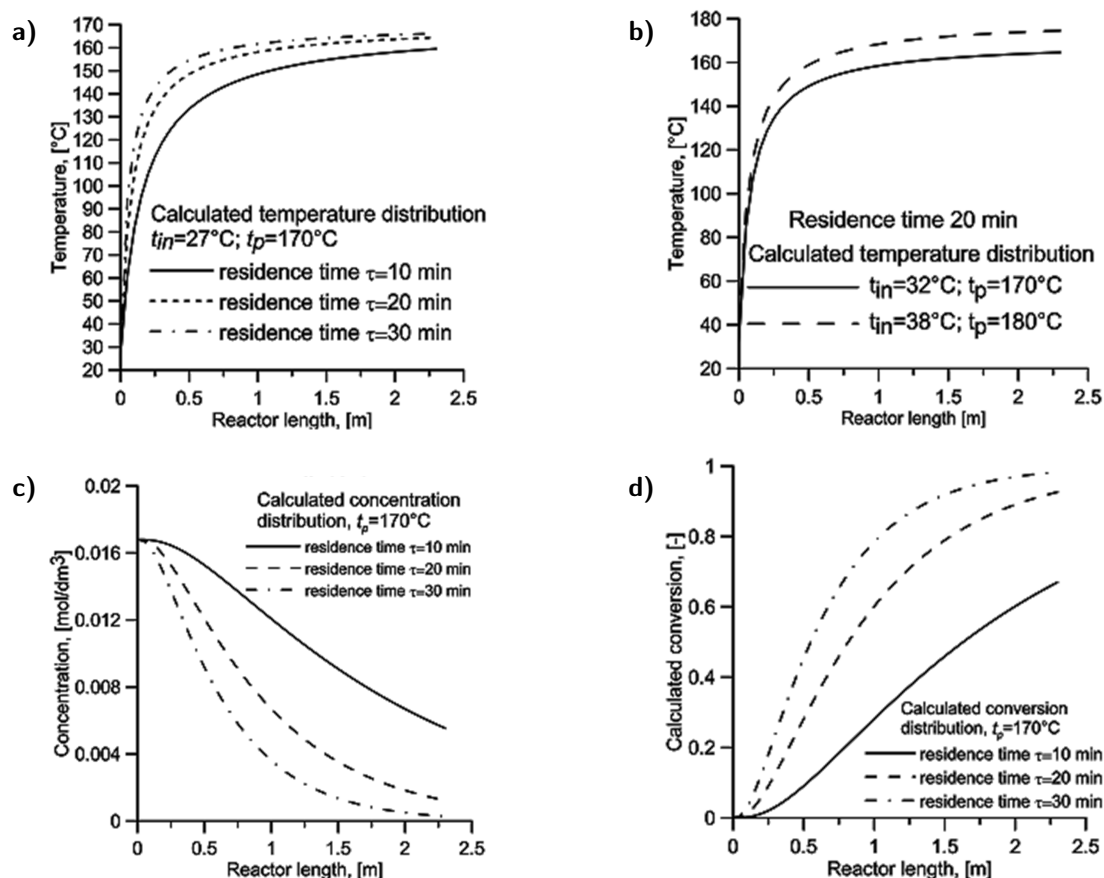


Figure 4. Predicted temperature, precursor concentration and conversion distributions during the flow of the reaction mixture through the reactor determined using a mathematical model of the process.

served. As expected, an increase in residence time induces an increase in the conversion of the AgNWs precursor, and the nature of these changes is non-linear.

Figure 5a shows a comparison of the measured and calculated conversion values and an indication of the capping agent (PVP) used. In most cases, discrepancies between observed and calculated values do not exceed  $\pm 15\%$ . For a residence

time of 10 min, the calculations produced underestimated values in all cases. Analysis of the reported results indicates that the molar mass of PVP has no significant effect on precursor conversion.

Figure 5b demonstrates a comparison of calculated and measured temperatures at the outlet of the reactor. The experimentally determined temperature values are approximately

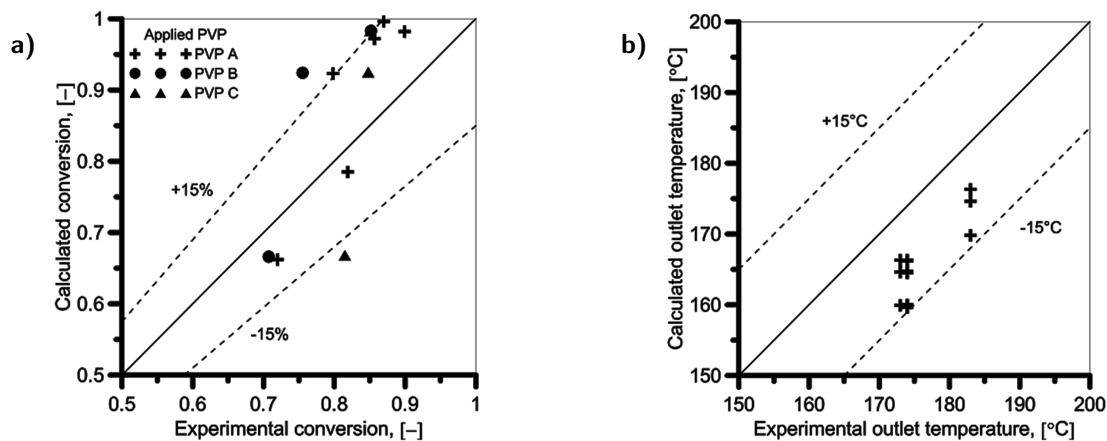


Figure 5. The comparison of calculated and observed: a) conversion values for PVP with different average molar weights; PVP A – 40 kDa; PVP B – 360 kDa, PVP C – 1300 kDa b) outlet reactor temperatures.

7–14 °C higher than those calculated in all cases analysed. This effect can presumably be attributed to the influence of radiation from the heating elements inside the laboratory dryer. Furthermore, the model's thermal balance equations neglect the energy effects associated with nucleation, growth and aggregation phenomena occurring during the synthesis of silver nanomaterials (Patakfalvi and Dékány, 2005). The influence and magnitude of these effects will be the subject of future research.

## 5. CONCLUSIONS

The applied simple mathematical model of the process makes it possible to determine the total conversion of the precursor with an error not exceeding  $\pm 20\%$ . The calculated outlet temperatures from the reactor are lower than those observed by 7–14 °C. It probably results from radiation heat transport inside the applied laboratory setup and the thermal effects accompanying nanomaterial formation in the polyol process. Further research is required to determine a more detailed kinetic equation for the AgNW formation process, which will consider the influence of additional factors, such as the amount of stabilising and mediating agents.

## ACKNOWLEDGEMENTS

Publication supported under the Rector's pro-quality grant. Silesian University of Technology, 04/030/RGJ22/0062.

## SYMBOLS

$c_p$	heat capacity, J/(kg·K)
$C_A$	concentration of silver nanowire precursor, mol/dm <sup>3</sup>
$d$	reactor I.D., m
$d_z$	reactor O.D., m
$D$	coil diameter, m
$E_A$	activation energy, J/mol
$\dot{G}$	a mass flow rate of the reaction mixture, kg/s
He	Helical number,
$k$	reaction rate constant, 1/s
$k_0$	pre-exponential factor, 1/s
$l$	length, m
Nu	Nusselt number, –
$p$	coil pitch ( $p = 0.01$ m), m
$R$	universal gas constant; $R = 8.314$ J/(mol·K), J/(mol·K)
Re	Reynolds number, –
$t$	temperature, °C
$u$	velocity, m/s
$V$	volume of the tubular reactor, m <sup>3</sup>
$\dot{V}$	volumetric flow rate, m <sup>3</sup> /s
$Q$	heat transfer rate, J/s
$X$	conversion, –

### Greek symbols

$\alpha$	heat transfer coefficient, W/(m <sup>2</sup> ·K)
$\lambda_t$	heat conductivity coefficient of reactor material; for silicon rubber $\lambda_t = 1$ W/m·K, W/m·K
$\sigma$	the Stefan–Boltzman constant; $\sigma = 5.67 \cdot 10^{-8}$ W/(m <sup>2</sup> ·K <sup>4</sup> ), W/(m <sup>2</sup> ·K <sup>4</sup> )
$\tau$	residence time, s

### Subscripts

0	refers to inlet condition
$c$	convection
$ge$	refers to the reaction mixture, ethylene glycol
$i$	local
in	inlet
out	outlet
$p$	refers to the reactor surroundings
$r$	radiation
$w$	inner wall of the reactor
$wz$	outer wall of the reactor

## REFERENCES

- Chen D., Qiao X., Qiu X., Chen J., Jiang R., 2010. Convenient, rapid synthesis of silver nanocubes and nanowires via a microwave-assisted polyol method. *Nanotechnology*, 21, 025607. DOI: [10.1088/0957-4484/21/2/025607](https://doi.org/10.1088/0957-4484/21/2/025607).
- Chou K.S., Hsu Ch.-Y., Liu B.-T., 2015. Salt-mediated polyol synthesis of silver nanowires in a continuous-flow tubular reactor. *RSC Adv.*, 5, 29872–29877. DOI: [10.1039/C5RA00320B](https://doi.org/10.1039/C5RA00320B).
- Doran P.M., 2013. *Bioprocess engineering principles*. 2nd edition, Academic Press, Waltham, 816–819. DOI: [10.1016/C2009-0-22348-8](https://doi.org/10.1016/C2009-0-22348-8).
- Dzido G., 2017. *Analiza wpływu pola mikrofalowego na charakterystykę nanocząstek srebra i tlenku miedzi otrzymanych w procesie przepływowym*. Wydawnictwo Politechniki Śląskiej, Gliwice, 117–123.
- Espinosa N., Søndergaard R.R., Jørgensen M., Krebs F.C., 2016. Flow synthesis of silver nanowires for semitransparent solar cell electrodes: A life cycle perspective. *ChemSusChem.*, 9, 893–899. DOI: [10.1002/cssc.201501437](https://doi.org/10.1002/cssc.201501437).
- Gottesman R., Tangy A., Oussadon I., Zitoun D., 2012. Silver nanowires and nanoparticles from a millifluidic reactor: application to metal assisted silicon etching. *New J. Chem.*, 36, 2456–2459. DOI: [10.1039/C2NJ40763A](https://doi.org/10.1039/C2NJ40763A).
- Ha H., Amicucci C., Matteini P., Hwang B., 2022. Mini review of synthesis strategies of silver nanowires and their applications. *Colloid Interface Sci. Commun.*, 50, 100663. DOI: [10.1016/j.colcom.2022.100663](https://doi.org/10.1016/j.colcom.2022.100663).
- Hemmati S., Barkey D.P., Eggleston L., Zukas B., Gupta N., Harris M., 2017. Silver nanowire synthesis in a continuous millifluidic reactor. *ECS J. Solid State Sci. Technol.*, 6, 144–149. DOI: [10.1149/2.0171704jss](https://doi.org/10.1149/2.0171704jss).
- Hobler T., 1979. *Ruch ciepła i wymienniki*. 5<sup>th</sup> edition, WNT, Warszawa, 523–525.

- Luu Q.N., Doorn J.M., Berry M.T., Jiang C., Lin C., May P.S., 2011. Preparation and optical properties of silver nanowires and silver-nanowire thin films. *J. Colloid Interface Sci.*, 356, 151–158. DOI: [10.1016/j.jcis.2010.12.077](https://doi.org/10.1016/j.jcis.2010.12.077).
- Manlapaz R.L., Churchill S.W., 1981. Fully developed laminar convection from a helical coil. *Chem. Eng. Commun.*, 9, 185–200. DOI: [10.1080/00986448108911023](https://doi.org/10.1080/00986448108911023).
- Nandikonda S., Davis E.W., 2011. Parameters affecting the microwave-assisted polyol synthesis of silver nanorods. *Int. Scholarly Res. Not.*, 2011, 104086. DOI: [10.5402/2011/104086](https://doi.org/10.5402/2011/104086).
- Patakfalvi R., Dékány I., 2005. Nucleation and growth of silver nanoparticles monitored by titration microcalorimetry. *J. Therm. Anal. Calorim.*, 79, 587–594. DOI: [10.1007/s10973-005-0583-z](https://doi.org/10.1007/s10973-005-0583-z).
- Senkara T., 1981. *Obliczenia cieplne pieców grzewczych w hutnictwie*. Wydawnictwo Śląsk, Katowice, 42–43.
- Yu J., Yang L., Jiang J., Dong X., Cui Z., Wang Ch., Lu Z., 2022. Scalable production of high-quality silver nanowires via continuous-flow droplet synthesis. *Nanomaterials*, 12, 1018. DOI: [10.3390/nano12061018](https://doi.org/10.3390/nano12061018).
- Zeng X., Zhou B., Gao Y., Wang C., Li S., Yeung C.Y., Wen W.J., 2014. Structural dependence of silver nanowires on polyvinylpyrrolidone (PVP) chain length. *Nanotechnology*, 25, 495601. DOI: [10.1088/0957-4484/25/49/495601](https://doi.org/10.1088/0957-4484/25/49/495601).
- Zhai X., Efrima S., 1996. Reduction of silver ions to a colloid by Eriochrome Black T. *J. Phys. Chem.*, 100, 1779–1785. DOI: [10.1021/jp951901a](https://doi.org/10.1021/jp951901a).